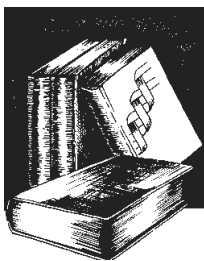


Structural basis for the antibacterial activity of the 12-membered-ring mono-sugar macrolide methymycin

Tamar Auerbach#, Inbal Mermershtain#, Anat Bashan,
Chen Davidovich, Haim Rozenberg, David H. Sherman¹
and Ada Yonath*

*Weizmann Institute of Science, Rehovot, Israel, and
¹Life Sciences Institute and Departments of Medicinal Chemistry,
Chemistry, Microbiology & Immunology, University of Michigan,
Ann Arbor, Michigan

**THIS COPY WAS CREATED BY THE
AUTHORS**



Structural basis for the antibacterial activity of the 12-membered-ring mono-sugar macrolide methymycin

Tamar Auerbach[#], Inbal Mermershtain[#], Anat Bashan, Chen Davidovich, Haim Rozenberg, David H. Sherman¹ and Ada Yonath^{*}

^{*}Weizmann Institute of Science, Rehovot, Israel, and

¹Life Sciences Institute and Departments of Medicinal Chemistry, Chemistry, Microbiology & Immunology, University of Michigan, Ann Arbor, Michigan

Structural basis for the antibacterial activity of the 12-membered-ring mono-sugar macrolide methymycin

Summary

The crystal structure of the complex of the large ribosomal subunit of the pathogen model *Deinococcus radiodurans* with the macrolide antibiotic methymycin, bearing a 12 membered macrolactone ring macrolide that contains a single amino sugar, shows that methymycin binds to the peptidyl transferase center (PTC) rather than to the high affinity macrolide binding pocket at the upper end of the ribosomal exit tunnel. This unexpected binding mode results in fairly efficient blockage of the 3' end of the A-site tRNA location, thus indicating the superiority of spatial-functional considerations over the formation of the typical high affinity macrolide interactions that due to the small size of methymycin could have led to incomplete blockage of the exit tunnel. Its binding involves rearrangements of several PTC nucleotides, some of which shown previously to be flexible. Comparisons between the binding modes of methymycin and other antibiotics are presented and discussed.

Key words:

methymycin, antibiotics, macrolides, ribosomes, X-ray crystallography, peptidyl transferase center.

Address for correspondence

Ada Yonath,
Life Sciences Institute
and Departments of
Medicinal Chemistry,
Chemistry, Microbiology
& Immunology,
University of Michigan,
Ann Arbor,
Michigan 48109;
e-mail:
ada.yonath@weizmann.ac.il

1. Introduction

Protein biosynthesis is a fundamental process in living cells. Among the many cellular components participating in it, the ribosome plays a key role, since it is the universal cellular organelle that acts as a nano-machine translating the genetic code into proteins. Ribosomes are composed of two riboprotein subunits of unequal size that associate upon initiation of the translation process and dissociate at its termination. Protein biosynthesis is performed cooperatively by both subunits. The small ribosomal subunit facilitates the initiation of the process and is involved in selecting the frame to be translated, decoding the genetic message, and controlling the fidelity of codon-anticodon interactions. The large ribosomal subunit forms the peptide bond, ensures smooth amino acid polymerization, and channels the nascent proteins through their exit tunnel. Genetic information is presented to the ribosome by messenger RNA (mRNA) and aminoacylated transfer RNA (tRNA) molecules deliver the amino acids. The ribosome possesses three tRNA binding sites. The A-site hosts the aminoacylated-tRNA, the P-site hosts the peptidyl tRNA, and the E-site designates the location of the exiting free tRNA once a peptide bond has been formed. The anticodon loops of the tRNAs are bound to the mRNA on the small subunit, and the 3' ends of the A- and P- tRNAs are located within the peptidyl transferase center (PTC), where the peptide bonds are being formed. The elongation is associated with A→P→E translocation by one codon of the mRNA together with the tRNA molecules bound to it. In each step of the elongation event the mRNA advances and a new peptide bond is formed between the amino acid bound to the A-site tRNA and the growing peptidyl bound to the P-site tRNA.

Antibiotics that target the ribosome perturb variant aspect of ribosome function. High resolution crystal structures of representatives of most of the families of structurally diverse ribosomal antibiotics complexed with ribosomal particles from eubacteria suitable to serve as pathogen models were recently determined. These structures showed that these antibiotics target ribosomes at distinct locations within functionally relevant sites and exert their inhibitory action utilizing diverse modes, thus elucidating basic concepts in antibiotic-binding modes at the molecular level (1,2) and providing tools to assess previous findings while developing ideas for novel antibiotic compounds. Particularly, individual ribosomal antibiotics compete with substrate binding, interfere with ribosomal dynamics, minimize ribosomal mobility, facilitate miscoding, hamper the progression of mRNA, block the nascent proteins exit tunnel, and prevent peptide bond formation.

Within the large ribosomal subunit the PTC is targeted by several antibiotics of diverse chemical nature, such as chloramphenicol, clindamycin, linezolid, lankacidin, the pleuromutilins and the streptogramins_A. The macrolides, ketolides, azalides and streptogramins_B, however, bind to a distinct pocket at the upper side of the protein exit tunnel and arrest progression of the nascent proteins. All members of this group display distinctive activity against bacteria (primarily Gram-positive) and

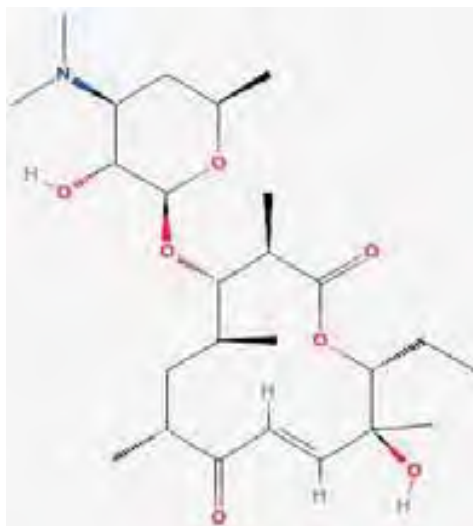


Fig. 1. The chemical formula of methymycin.

mycoplasma. Common to all macrolides and their structural analogs are two indispensable chemical components: a substituted macrolactone (polyketide) ring, to which at least one sugar moiety (typically possessing an amino group) is covalently linked. Among the members of this group methymycin bears the smallest macrolactone ring (Fig. 1), and thus we were motivated to assess its ribosomal binding characteristics as a basis for its biological activity.

Methymycin, ($C_{25}H_{43}NO_7$) molecular weight of 469.6 (3), is the smallest known macrolide that includes a 12 membered ring macrolactone as opposed to the commonly used macrolides (e. g. erythromycin, tylosin) that are comprised of 14- or 16-membered macrolactone rings. In addition, methymycin contains only one sugar moiety, instead of two or more sugars that are typical of many macrolides. The 12-membered ring aglycone of methymycin (10-deoxymethynolide) is the product of the *pik* PKS gene cluster from *Streptomyces venezuelae*, which represents a well characterized natural product system (4). Thorough investigation of the genetic and biochemical nature of this system (e.g. 5,6) led to advanced understanding of polyketide biosynthesis, which, in turn, stimulated the design of recombinant PKS genes, capable of efficient production of diverse compounds with various macrolactone rings and sugar systems (7,8). This attractive technology is based on the transfer of biosynthetic genes from the original producers to a robust heterologous host for use in construction of combinatorial biosynthetic systems (9-11). This methodology has been further developed by the replacement of the widely used relatively slow *Streptomyces coelicolor* (12) and *Streptomyces lividans* (13), by another member of the same family, namely *Streptomyces venezuelae* (14-16) that involves a shorter culture period for the production of large quantities of metabolites (17-20).

In contrast to the typical 14-membered macrolactone ring macrolides (e.g. erythromycin, clarithromycin, and roxithromycin) and their derivatives with 15 (azi-

thromycin) or 16 (e.g. tylosin) membered ring, methymycin possesses a ring with 12 members only. Additionally, all of the above mentioned macrolides possess at least two sugar moieties, whereas only a single sugar, namely the aminosugar desosamine, is bound to the methymycin macrolactone. Despite these substantial chemical differences, methymycin displays antibiotic activity against Gram-positive bacteria, similar to typical and larger macrolide antibiotics.

Interestingly, methymycin resistance mechanisms appear to differ from the typical mechanisms that acquire macrolide resistance by modifications of the 23S rRNA nucleotide at position 2058: the mutation A2058G (21) and *erm*-encoded methylation that transforms the 2058 adenine into ⁶N, ⁶N-dimethyladenine (22). Four types of responses to macrolides binding were identified regarding *erm* gene induction of antibiotic resistance: full induction by 14-membered-ring macrolides (e.g. erythromycin); selective induction by 16-membered-ring macrolides (e.g. tylosin); selective induction by the 14-membered-ring macrolide megalomicin; no induction by the 12-membered-ring macrolide methymycin. Consequently, assuming that all macrolides bind to the same binding pocket at the protein exit tunnel, the efficiency of the induction of *erm* methyltransferases gene expression was correlated with the macrolide size (23).

To shed light on the binding of methymycin to the ribosome, identify its key interactions, and address the lack of correlation between its binding and induction of *erm* gene expression, we determined the high-resolution X-ray structure of the complex of the large (50S) ribosomal subunit of the eubacterium *Deinococcus radiodurans* complexed with clinically relevant concentration of methymycin. Here we report the molecular details of methymycin interactions with the large ribosomal subunit and discuss the unexpected results of these studies, which suggest that despite the availability of a high affinity pocket, steric considerations and their consequent increase in inhibition efficiency dominate the mode of methymycin binding.

2. Methods

Soaking crystals and X-ray diffraction data collection: Crystals were grown as in (24) and soaked in solutions containing 0.025mM of methymycin for 8 hours at 20° C, transferred into cryo-buffer and shock-frozen in liquid nitrogen. Data were collected from shock-frozen crystals with synchrotron radiation beam at ID23-1/2, ESRF.

Data Processing: Data processing and scaling was performed using the HKL2000 package (25). Crystals of D50S belong to the space group I222 and contain one particle per asymmetric unit. The native structure of D50S was refined against the structure factor amplitudes of the antibiotic complex using rigid body refinement as implemented in CNS (26). For free R-factor calculation, random 5% of the data were omitted during refinement. The antibiotic site was readily determined from sigma weighted difference maps. To obtain an unbiased electron density map, the 23S

rRNA environment of the binding site has been omitted from the calculations. To enhance the details, the difference maps were subjected to density modification using the CCP4 package suite (27). The resulting electron differences map revealed unambiguously the position and orientation of the antibiotic. Methymycin initial structure was generated with the program ChemDraw and was fitted manually into the electron density map. Finally the complete structure was subjected to energy minimization with CNS. The ribosome-antibiotic interactions were determined with LigPlot (28) and LPC (29).

3. Results and Discussion

The crystal structure, determined at 3.7Å resolution (Tab. and Fig. 2) enabled methymycin localization in the large ribosomal subunit, and illuminated the structural basis for its inhibitory action. Common to all macrolides and all PTC antibiotics, methymycin interacts solely with rRNA. However, in contrast to the 14-16 membered ring macrolides (21,30-32), their advanced derivatives, azalides and ketolides (33,34) and the streptogramin_B component of the synergetic drug, synergid (35), which bind to the high affinity pocket located at the upper side of the tunnel, methymycin binds to the PTC, although it possesses both moieties known to facilitate macrolides binding to their typical pocket.

Table

Crystallographic and refinement data

Crystal Parameters	
Space group	<i>I</i> 222
Cell Dimensions (Å)	172.5 × 415.7 × 701.7
Resolution (Å)	40-3.7 (3.88-3.73)
No. of unique reflections	241,239 (22,816)
Completeness (%)	96.0 (95.0)
Rsym (%)	16.7 (78.7)
No. of crystals merged	3
I/σ(I)	6.4 (1.6)
Redundancy	5.6(5.4)
Refinement Statistics:	
R/Rfree (%)	28.4/35.1
Rms deviation from ideal Bond length (Å)	0.09
Rms deviation from ideal Bond angles	1.47

Values for the highest resolution bin are shown in brackets.

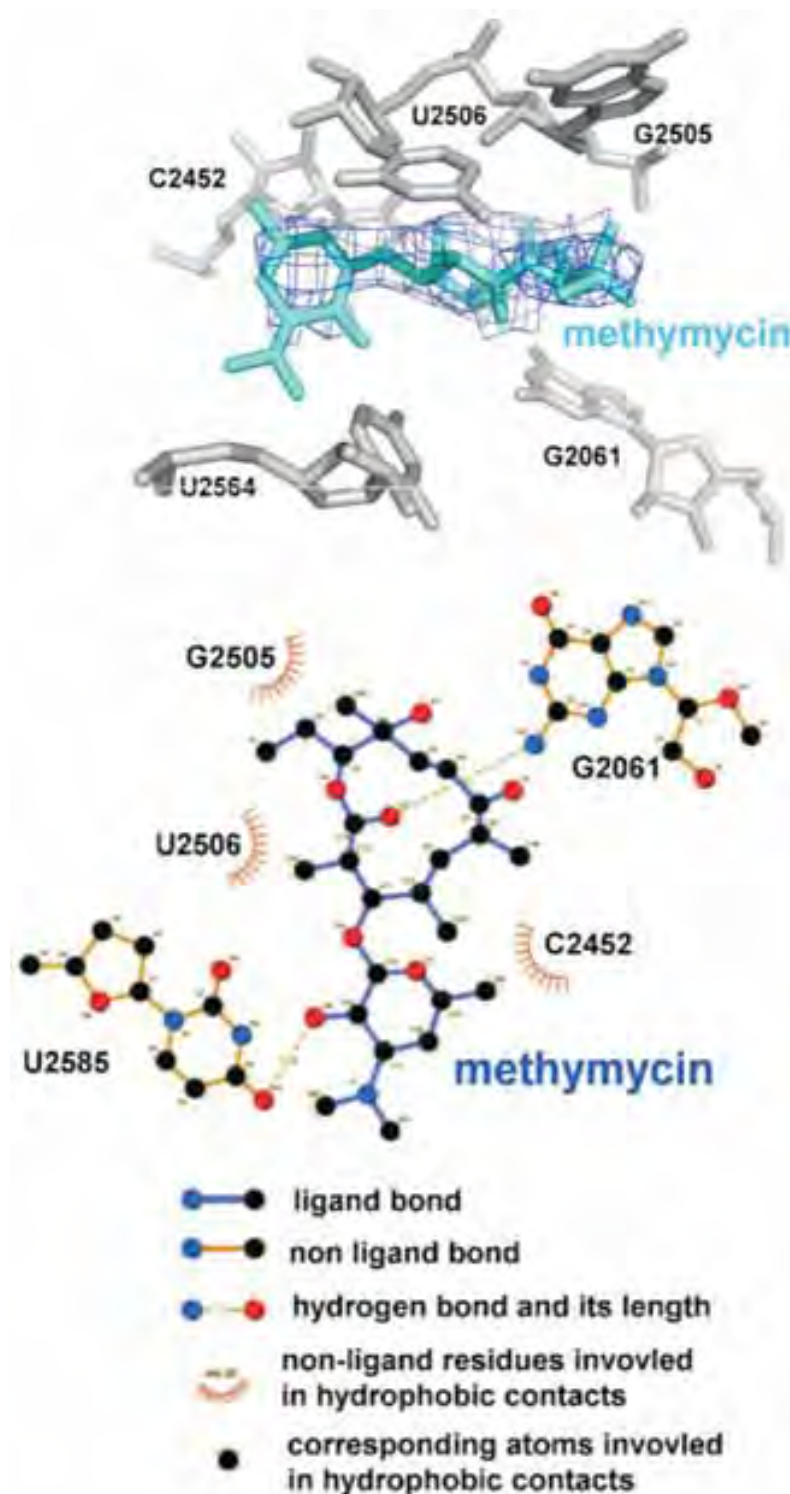


Fig. 2. **Top:** $F_o - F_c$ sigma weighted electron density map, contoured at 1 sigma level. **Bottom:** the interactions of methymycin with the ribosome, as determined by LigPlot.

The unique mode of methymycin binding can be rationalized by its consequent efficiency in ribosome inhibition, compared to the expected limited blockage if methymycin was bound to the typical macrolide binding pocket. The attachment of this

unusually small macrolide to the rather crowded PTC instead of to the larger free space of the exit tunnel should be more useful for inhibition of protein biosynthesis. The preference of functional productivity indicates the superiority of spatial and inhibitory considerations over the formation of high affinity interactions at the macrolides binding pocket.

Recent studies of natural and unnatural macrolide antibiotics against a variety of bacterial targets (S. Li, and D. H. Sherman, to be published) showed that methymycin possesses significant inhibitory power, with MIC (minimum inhibitory concentration) of 8 $\mu\text{g/ml}$ against *D. radiodurans*. These studies verified the crystal structure (Fig. 2) that revealed that methymycin interacts with PTC nucleotides via a network of hydrogen bonds and hydrophobic contacts involving the macrolactone ring and the desosamine moiety, in accord with findings showing that without the sugar component methymycin is biologically inactive (36). Specifically, two hydrogen bonds could be clearly identified: one between OH6 of the sugar moiety of methymycin and O4 of U2585 (*E. coli* nomenclature throughout) and the second between O2 of methymycin and N2 of G2061. Nucleotides involved in hydrophobic contacts include C2452, G2061, G2505, U2506 and U2585.

Comparison of the location of methymycin in the PTC against positions observed for other PTC antibiotics bound to the large ribosomal subunit of the same eubacterium, *D. radiodurans*, namely chloramphenicol, clindamycin (30), the streptogramin_A component of synergid (24) and the pleuromutilins (37), showed various levels of overlap, and indicated that the main inhibitory function of methymycin is interfering with accommodation of the A-site tRNA, as its binding site overlaps the position of the 3' end of the A-site tRNA (38) (Fig. 3).

Similar to most of the PTC antibiotics, particularly the pleuromutilins (37), and also chloramphenicol (30) and streptogramin_A (35), methymycin binding induces substantial rearrangement of the ribosomal nucleotides residing in its vicinity (Fig. 4). Some of these motions propagate towards more remote locations, such as nucleotides residing in the second or third shells around the bound drug. Specifically, the following nucleotides moved away from their positions in the native D50S upon methymycin binding: U2585, U2506, C2452, U2504 and G2505. As a consequence, two flexible nucleotides of the internal PTC shell stack to two second shell nucleotides: G2505 to G2576 and A2503 to A2059. Interestingly, A2453 of the second shell moved away, in the opposite direction, as a consequence of the rearrangement of C2452. Similar motions, in the opposite direction, were observed also for U2584, G2447 and A2602 that undergoes a 45° rotation.

A2602 is located 10 Å away from methymycin binding site. It is one of the most flexible nucleotides in and around the PTC (reviewed in (39)). Its outstanding flexibility is demonstrated by its ability to swing by up to 180° upon binding substrates, factors, antibiotics, or inhibitors, even when examining solely the eubacterial domain (24,40-43). It plays an important role in the rotational motion element of the translocation of the A-site tRNA, the key activity facilitating the polymerase function

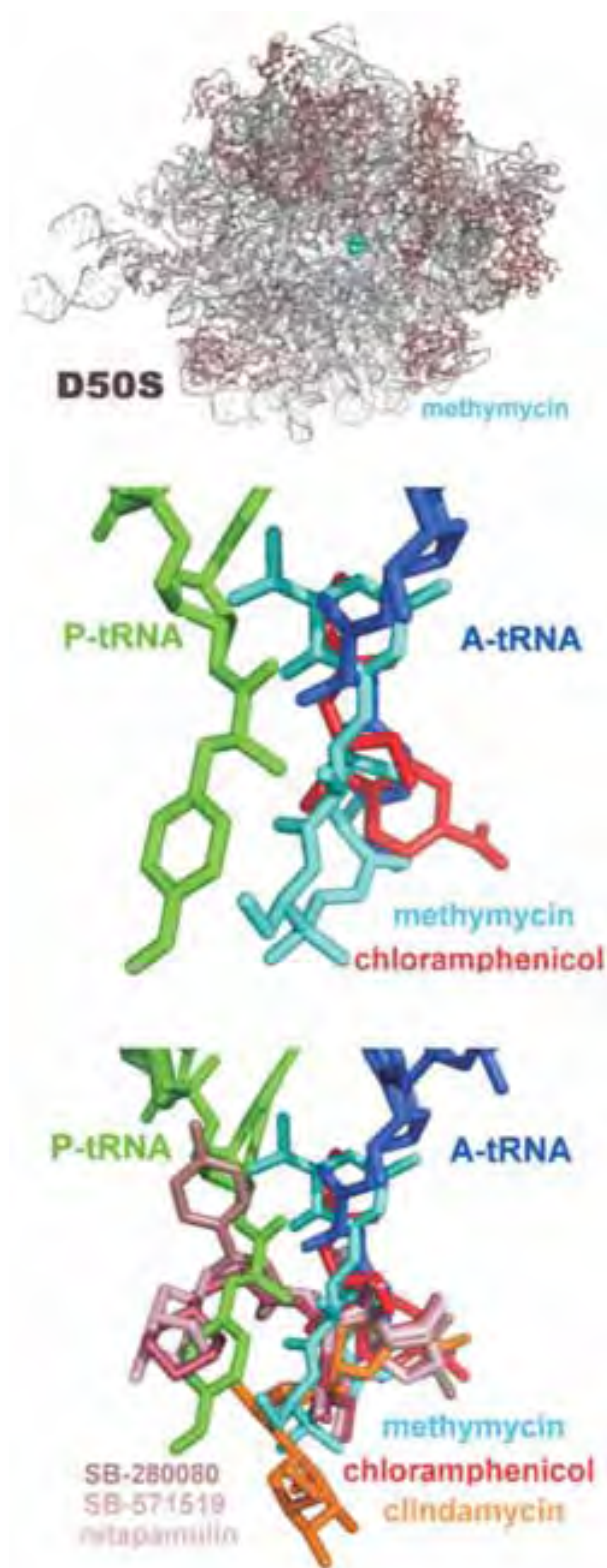


Fig. 3. The position of methymycin within the large ribosomal subunit. The 3'ends of A- and P-site tRNAs (38) are shown for orientation.

Top: methymycin binds to the PTC (not to the tunnel).

Middle and bottom: methymycin position within the PTC, compared to other PTC antibiotics, namely chloramphenicol, clindamycin (30) and three pleuromutilins (37).

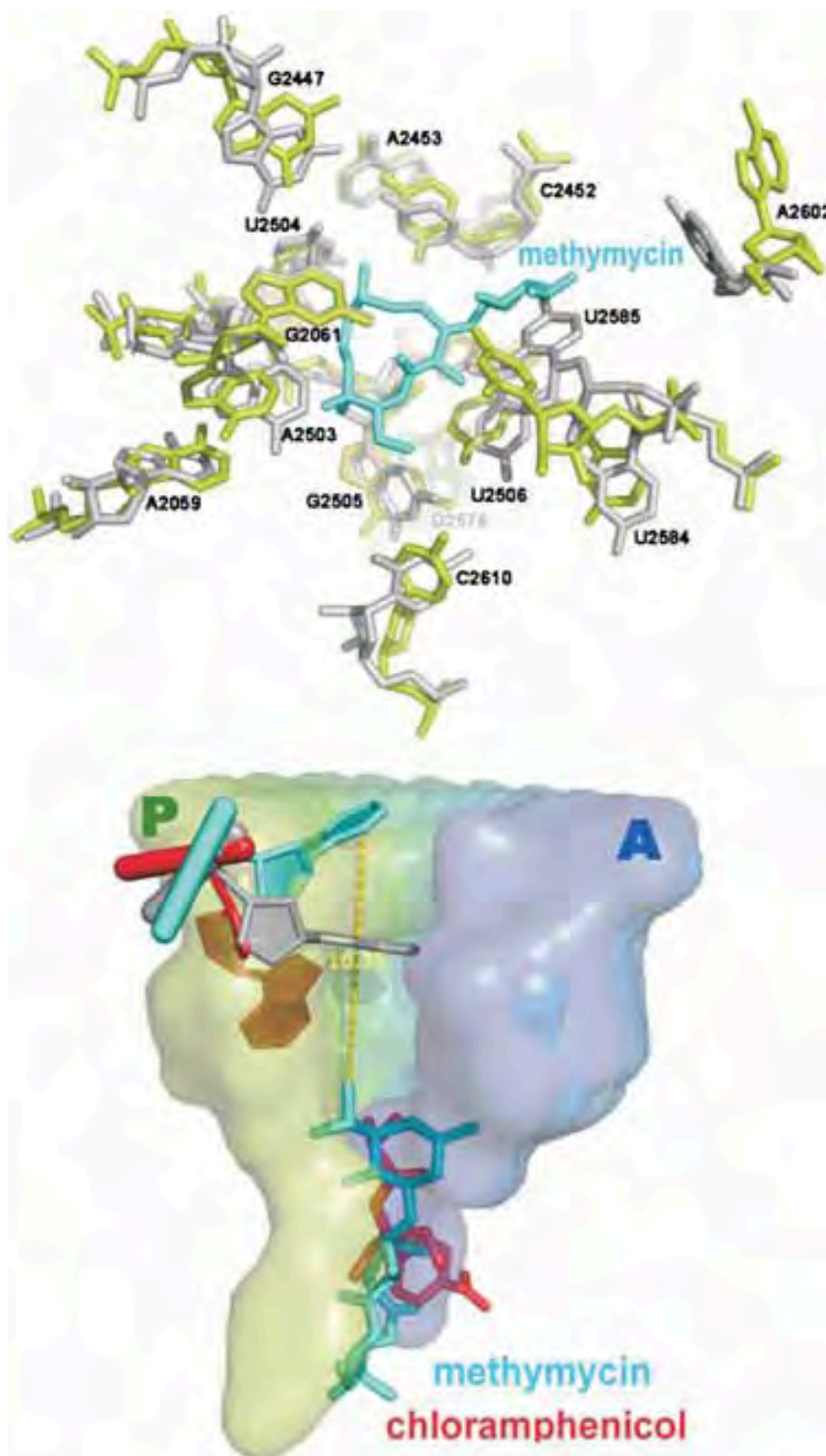


Fig. 4. **Top:** Alterations in the orientations of PTC nucleotides upon methymycin binding
Bottom: the dramatic motion of A2602 occurring upon methymycin or chloramphenicol (30) binding despite its remote position. The volume occupied by the A- to P-site translocation of A-site tRNA 3' end is shown by the half transparent surface. The motion is represented by a gradual transition from blue to green. The letters A and P designate the approximate positions of A-site tRNA and P-site tRNA at the beginning and the end of the translocation, respectively (38,44).

of the ribosome, namely the synthesis of the nascent protein. This translocation is a combination of two independent, albeit synchronized motions: the sideways shift, performed as part of the overall mRNA/tRNA translocation, and a rotatory motion of the A-tRNA 3' end along a path confined by the PTC (38,44). The dramatic alteration in the orientation of A2602 upon methymycin binding indicates that binding alone can lead, *via* a chain of nucleotides movements, to a swing motion of A2602. This swinging fixes A2602 in a nonproductive orientation, similar to the effect of chloramphenicol binding. Thus, it seems that the modes of action of both methymycin and chloramphenicol are composed of two components: blockage of the A-site at the PTC and the induction of a non-productive orientation of A2602, namely the interruption of the A-site tRNA translocation (Fig. 4).

The overlap between methymycin and chloramphenicol (Fig. 3) extend beyond the similarities in blocking the A-site and the indirect alteration of A2602 orientation. Thus, although their positioning and interaction networks are somewhat different, presumably because methymycin is bulkier, both make a hydrogen bond with G2061. This nucleotide is at the same position in native D50S, as well as in its complexes with chloramphenicol. It is also the nucleotide that interacts with all of the pleuromutilins. U2504, C2452 and C2453 have moved away from their native position upon binding chloramphenicol as well as methymycin. However, other nucleotides behave differently. Among them, the final orientations of the highly flexible U2585 and A2602 are different. Whereas chloramphenicol does not trigger conformational reengagement of U2585, this nucleotide moves away from its native position upon methymycin binding, probably due its bulkier volume, and the hydrogen bond that is formed between methymycin and U2585 seems to minimize the flexibility of this nucleotide during translocation. Moreover, A2602 moves towards chloramphenicol whereas it moves away from its native position upon methymycin binding (Fig. 4). Similarly, G2583 moves towards chloramphenicol, whereas it moves away from its native position upon methymycin binding and C2610 moves towards methymycin, but away from its native position upon chloramphenicol binding.

Acknowledgments

Thanks are due to all members of the ribosome group at the Weizmann Institute and the bioorganic chemistry group at the Life Sciences Institute and Department of Medicinal Chemistry at the University of Michigan. Crystallographic data were collected from at ESRF, Grenoble, France, stations ID23-1 and ID23-2. Support was provided by the US National Institutes of Health to DHS (GM076477) and AY (GM34360) and by the Kimmelman Center for Macromolecular Assemblies to AY. CD is supported by the Adams Fellowship Program of the Israel Academy of Sciences and Humanities and AY holds the Martin and Helen Kimmel Professorial Chair.

Literature

1. Bashan A., Yonath A., (2008), *Trends Microbiol* 16, 326-335.
2. Yonath A., (2005), *Annu. Rev. Biochem.*, 74, 649-79.
3. Buckingham J., (1996), *Dictionary of Natural Products*.
4. Xue Y., Zhao L., Liu H. W., Sherman D. H., (1998), *Proc. Natl. Acad. Sci. USA*, 95, 12111-12116.
5. Borisova S. A., Zhao L., Sherman D. H., Liu H. W., (1999), *Org. Lett.*, 1, 133-136.
6. Zhao L., Que N. L. S., Xue Y., Sherman D. H., Liu H. W., (1998), *J. Am. Chem. Soc.*, 120, 12159-12160.
7. Xue Q., Ashley G., Hutchinson C. R., Santi D. V., (1999), *Proc. Natl. Acad. Sci. USA* 96, 11740-11745.
8. Lee S. K., Basnet D. B., Hong J. S. J., Jung W. S., Choi C. Y., Lee H. C., Sohng J. K., Ryu K. G., Kim D. J., Ahn J. S., Kim B. S., Oh H. C., Sherman D. H., Yoon Y. J., (2005), *Adv. Synth. Catal.*, 347, 1369-1378.
9. Pfeifer B. A., Khosla C., (2001), *Microbiol. Mol. Biol. Rev.*, 65, 106-118.
10. Rude M. A., Khosla C., (2004), *Chem. Eng. Sci.*, 59, 4693-4701.
11. Wenzel S. C., Muller R., (2005), *Curr. Opin. Biotechnol.*, 16, 594-606.
12. McDaniel R., Thamchaipenet A., Gustafsson C., Fu H., Betlach M., Ashley G., (1999), *Proc. Natl. Acad. Sci. USA*, 96, 1846-1851.
13. Ziermann R., Betlach M. C., (1999), *Biotechniques*, 26, 106-110.
14. Yoon Y. J., Beck B. J., Kim B. S., Kang H. Y., Reynolds K. A., Sherman D. H., (2002), *Chem. Biol.*, 9, 203-214.
15. Jung W. S., Kim E. S., Kang H. Y., Choi C. Y., Sherman D. H., Yoon Y. J., (2003), *J. Microbiol. Biotechnol.*, 13, 823-827.
16. Hong J. S. J., Park S. H., Choi C. Y., Sohng J. K., Yoon Y. J., (2004), *FEMS Microbiol. Lett.*, 238, 291-399.
17. Zhao L. S., Ahlert J., Xue Y. Q., Thorson J. S., Sherman D. H., Liu H. W., (1999), *J. Am. Chem. Soc.*, 121, 9881-9882.
18. Xue Y., Sherman D. H., (2000), *Nature*, 403, 571-575.
19. Wilson D. J., Xue Y., Reynolds K. A., Sherman D. H., (2001), *J. Bacteriol.*, 183, 3468-3475.
20. Xue Y., Sherman D. H., (2001), *Metab. Eng.*, 3, 15-26.
21. Sigmund C. D., Ettayebi M., Morgan E. A., (1984), *Nucleic Acids Res.*, 12, 4653-4663.
22. Weisblum B., (1995), *Antimicrob. Agents. Chemother.*, 39, 577-585.
23. Kamimiya S., Weisblum B., (1997), *Antimicrob. Agents. Chemother.*, 41, 530-534.
24. Harms J., Schluenzen F., Zarivach R., Bashan A., Gat S., Agmon I., Bartels H., Franceschi F., Yonath A., (2001), *Cell*, 107, 679-688.
25. Otwinowski Z., Minor W., (1997), in: *Macromolecular Crystallography*, Eds. Carter J. C. W., Sweet R. M., Vol. 276, 307-326.
26. Brunger A. T., Adams P. D., Clore G. M., DeLano W. L., Gros P., Grosse-Kunstleve R. W., Jiang J. S., Kuszewski J., Nilges M., Pannu N. S., Read R. J., Rice L. M., Simonson T., Warren G. L., (1998), *Acta Crystallogr. D Biol. Crystallogr.*, 54, 905-921.
27. CCP4, (1994), *Acta Crystallogr. D Biol. Crystallogr.*, 50, 760-763.
28. Wallace A. C., Laskowski R. A., Thornton J. M., (1995), *Protein Eng.*, 8, 127-134.
29. Sobolev V., Sorokine A., Prilusky J., Abola E. E., Edelman M., (1999), *Bioinformatics*, 15, 327-332.
30. Schluenzen F., Zarivach R., Harms J., Bashan A., Tocilj A., Albrecht R., Yonath A., Franceschi F., (2001), *Nature*, 413, 814-821.
31. Berisio R., Schluenzen F., Harms J., Bashan A., Auerbach T., Baram D., Yonath A., (2003), *Nat. Struct. Biol.*, 10, 366-370.
32. Pyetan E., Baram D., Auerbach-Nevo T., Yonath A., (2007), *Pure Appl. Chem.*, 79, 955-968.
33. Schluenzen F., Harms J. M., Franceschi F., Hansen H. A., Bartels H., Zarivach R., Yonath A., (2003), *Structure*, 11, 329-38.
34. Berisio R., Harms J., Schluenzen F., Zarivach R., Hansen H. A., Fucini P., Yonath A., (2003), *J. Bacteriol.*, 185, 4276-4279.
35. Harms J., Schluenzen F., Fucini P., Bartels H., Yonath A., (2004), *BMC Biol.*, 2, 4, 1-10.

36. Kao C. L., Borisova S. A., Kim H. J., Liu H. W., (2006), *J. Am. Chem. Soc.*, 128, 5606-5607.
37. Davidovich C., Bashan A., Auerbach-Nevo T., Yaggie R. D., Gontarek R. R., Yonath A., (2007), *Proc. Natl. Acad. Sci. USA*, 104, 4291-4296.
38. Bashan A., Agmon I., Zarivach R., Schluenzen F., Harms J., Berisio R., Bartels H., Franceschi F., Auerbach T., Hansen H. A. S., Kossoy E., Kessler M., Yonath A., (2003), *Mol. Cell.*, 11, 91-102.
39. Yonath A., (2003), *Biol. Chem.*, 384, 1411-1419.
40. Korostelev A., Trakhanov S., Laurberg M., Noller H. F., (2006), *Cell*, 126, 1065-1077.
41. Yusupov M. M., Yusupova G. Z., Baucom A., Lieberman K., Earnest T. N., Cate J. H., Noller H. F., (2001), *Science*, 292, 883-896.
42. Schuwirth B. S., Borovinskaya M. A., Hau C. W., Zhang W., Vila-Sanjurjo A., Holton J. M., Cate J. H. D., (2005), *Science*, 310, 827-834.
43. Selmer M., Dunham C. M., Murphy Iv. F. V., Weixlbaumer A., Petry S., Kelley A. C., Weir J. R., Ramakrishnan V., (2006), *Science*, 313, 1935-1942.
44. Agmon I., Bashan A., Zarivach R., Yonath A., (2005), *Biol. Chem.*, 386, 833-844.